



**HAL**  
open science

# Schwarz Waveform Relaxation and Krylov Accelerators for Reactive Transport

Florian Haeberlein, Laurence Halpern, Anthony Michel

► **To cite this version:**

Florian Haeberlein, Laurence Halpern, Anthony Michel. Schwarz Waveform Relaxation and Krylov Accelerators for Reactive Transport. 2015. hal-01384281

**HAL Id: hal-01384281**

**<https://hal.science/hal-01384281v1>**

Preprint submitted on 20 Oct 2016

**HAL** is a multi-disciplinary open access archive for the deposit and dissemination of scientific research documents, whether they are published or not. The documents may come from teaching and research institutions in France or abroad, or from public or private research centers.

L'archive ouverte pluridisciplinaire **HAL**, est destinée au dépôt et à la diffusion de documents scientifiques de niveau recherche, publiés ou non, émanant des établissements d'enseignement et de recherche français ou étrangers, des laboratoires publics ou privés.

# Schwarz Waveform Relaxation and Krylov Accelerators for Reactive Transport

Florian Haeberlein\*    Laurence Halpern†    Anthony Michel‡

October 19, 2016

## Abstract

In this work we propose new algorithms for space time nonlinear reactive transport. They conjugate the versatility of Optimized Schwarz Waveform Relaxation, permitting adaptive time stepping, see [1, 12], and the fast convergence of Newton algorithms, see [6]. We present three approaches which differ in the order of combination of Newton's method and the Schwarz waveform relaxation algorithm. In the new approaches, the arising linear systems are treated by an inexact Krylov-type method. Numerical tests in 2D study the influence of the parameter of the Robin transmission condition. They prove that both approaches provide a considerable acceleration of the convergence speed. We provide also results in 3D for a two species nonlinear coupled reactive transport system in the context of CO<sub>2</sub> geological storage simulation.

MSC: 65B99, 65F08, 65N55, 65Y05

**Keywords:** multi-species reactive transport, global implicit approach, time-space domain decomposition, optimised Schwarz Waveform Relaxation, CO<sub>2</sub> geological storage, high performance computing.

**Acknowledgment:** this work was supported by the research french agency ANR (project SHP-CO<sub>2</sub>).

## 1 Introduction

Scientists commonly agree to the indeed existing impact of CO<sub>2</sub> on the greenhouse effect. The transition from classical, (*i.e.* fossil-based), to renewable energy sources has already begun, nevertheless, they still did not exceed 3.5 % on a global level see <http://www.iea.org/publications/freepublications/publication/KeyWorld2014.pdf>. As a consequence, in the next decades, our energy will mainly be supplied by fossil

---

\*LAGA, UMR 7539 CNRS, Université Paris 13, 93430 Villetaneuse, FRANCE, [florian.haeberlein@yahoo.fr](mailto:florian.haeberlein@yahoo.fr)

†LAGA, UMR 7539 CNRS, Université Paris 13, 93430 Villetaneuse, FRANCE, [halpern@math.univ-paris13.fr](mailto:halpern@math.univ-paris13.fr)

‡IFP Energies nouvelles, 1 et 4 avenue de Bois-Préau, 92852 Rueil-Malmaison, France, [anthony.michel@ifpen.fr](mailto:anthony.michel@ifpen.fr)

fuels.

Carbon Capture and Storage (CCS) is seen as a promising way to ensure the transition from fossil based to renewable energy: on the one hand, it allows to keep existing infrastructures in and use the gained know-how on fossil power plants. On the other hand, it allows to provide necessary time to develop experience and build infrastructure in the relatively new field of renewable energies.

The CCS approach separates  $\text{CO}_2$  from other gases during the energy production process and transforms it into a supercritical or liquid state. It is then eventually transported for short distances by pipelines to the injection well, where it is injected in the subsurface.

During and after injection of  $\text{CO}_2$  into saline aquifers, several physical and chemical processes appear. The injected  $\text{CO}_2$  dissolves partially in water and changes the pH, the water becomes acid and attacks the rock matrix. This changes the geophysical system, e. g. important changes in the porosity and permeability and hence in the way of how the aquifer moves. In order to ensure the reliability of the technical processes and the consequent changes in the subsurface system, a preprocessing numerical simulation has to be undertaken in order to predict it numerically.

Reactive transport models can be used for large field of applications,  $\text{CO}_2$  geological storage simulation is only one of them. Those models can be represented by a system of time-dependent transport equations modelled by partial differential equations which are coupled by nonlinear functions that represent the source terms resulting from chemical reactions. In this paper, we concentrate on a two species reactive transport system which is a subsystem of the multispecies reactive transport system presented in [16, 10].

The numerical simulation of such reactive transport models in the context of  $\text{CO}_2$  geological storage is a quite challenging task. This is mainly due to two different issues. On the one hand, the aim of the simulation is to provide information on a large area within a long time period in order to ensure the reliability of the storage process. The regarded scales are tremendously large, i. e. the interesting time scale is hundreds and even thousands of years and some hundreds of kilometres in space. On the other hand, the characteristics of the problem itself which contains highly different time scales and quite different levels of numerical complexity.

For the discretisation of the partial differential equations, finite volumes and close methods have established themselves for different reasons. On the one hand, they are easy to code, they work on very general meshes which are often based more on geological than on mathematical criteria, and they provide naturally interesting properties like flux conservation which is highly desirable in this context, see [8]. Nevertheless, all different classes of methods lead to a large system of algebraic equations which are nonlinear, due to chemical coupling terms. Efficient approaches to solve those problems have been developed and tested in different applications. Robust and fast methods are now available which combine nonlinear and linear solvers and which have only frugal need of memory capacity (e. g. Jacobian-free Newton-Krylov methods, see [15]). With the new generation of multicore-multiprocessor computers, new parallel algorithms, based on domain decomposition in space, appeared, designed for linear and nonlinear problems (see the books [22, 23, 20] and [18] in this context).

Nonetheless, besides the development in the previously mentioned fields, there are several issues, which have not been solved. One important field is the heterogeneity in space and time. As it has been mentioned, only a small part of the simulation domain

is highly reactive while most of the domain is close to an equilibrium state. The chemical reactivity reflects in strong nonlinear coupling terms which have an impact on the nonlinear solver. Usually, there are two ways out of this problem. Either, one accepts a high number of iterations in the nonlinear solver with the risk that no convergence can be achieved. Or, one adapts the time step in order to ensure faster convergence with higher probability. In practice, the second choice is done since this is the a good compromise between higher costs and convergence probability. Cutting the time step is quite easy when it is done globally. But, as the reason for cutting the time step is localised, the time step should be cut only locally. Otherwise, the part of the simulation domain, which is not dominated by strong nonlinearities is solved with a much higher precision than needed.

In the context of CCS, it is also important to be able to use different mesh sizes and different time steps in some parts of the computational domains. The Schwarz waveform relaxation (SWR) methods are in their own conception able to deal with different time steps in different subdomains. The domain is split in several subdomains and the numerical approximation is done over a whole time window, iteratively on the subdomains which are coupled by transmission conditions. The choice of the transmission conditions is a crucial issue in order to achieve high-performing algorithms. So called Robin or Fourier transmission conditions, or even second order operators (Ventcel type) have proven to produce much faster algorithms than the “classical“ Schwarz boundary operator, for which Dirichlet data exchange the informations between neighbouring subdomains. A procedure for the optimization of the coefficients has been set, theoretical and numerical results have been produced in the last decade, for the linear advection-diffusion-reaction equation, see [13, 1]. An analysis of the optimized transmission conditions to be used for the two species reactive transport system considered here can be found in [11]. Note that these algorithms are efficient for overlapping or nonoverlapping subdomains. They can very well handle the coupling between two different models with different space and time steps, see [14] for an ocean-atmosphere coupling.

The Schwarz waveform relaxation algorithm for nonlinear problems has been analysed in various frames, first for sublinear problems, see [9]. Optimized Schwarz waveform relaxation algorithm, with nonlinear transmission conditions were first introduced in [14], for the semilinear wave equation. In [5], the semilinear advection-diffusion reaction equation in two dimensions was considered,  $\partial_t u - \nu \Delta u + f(u) = 0$ , where  $f$  is constrained only to be in  $C^2(\mathbb{R})$ , with  $f(0) = 0$ . Nonoverlapping Robin-Schwarz and Ventcell-Schwarz were proposed and analyzed. The main difficulty in this case is that each iterate in a subdomain is solution of a nonlinear problem, whose solution has to be defined properly, and has its own time of existence  $T_j^n$ , where  $j$  is the number of the subdomain, and  $n$  the number of the iterate. The sequence  $(T_j^n)_n$  is decreasing, and it has been shown that there is a lower bound  $T_*$  for these times. Then the convergence is achieved inside  $(0, T_*)$ . From a numerical point of view, a nonlinear system has to be solved in each subdomain at every step, which has been implemented with  $\mathbf{P}_1$  finite elements in space, and a linearly implicit Euler scheme in time. It turns out that the requirement of small time interval given by the existence analysis is not compelling. Furthermore nonlinear transmission condition where the coefficients  $p$  and  $q$  depend on the iterates through the formulas of [1] were successfully implemented. For the nonlinear reactive transport system, with suitable assumptions on the coefficients, a similar analysis holds, this is the *Classical Approach* we introduce precisely in §3.

However, there is still space for acceleration.

Before optimised transmission conditions have been in the spotlight, either different overlap sizes of the subdomains (see [2] for a detailed study of the influence of the overlap size) and/or Krylov-type methods like BiCGStab ([24]) or GMRES ([21]) have been applied in order to accelerate the convergence of Schwarz-type methods independently of the chosen transmission conditions. Brakkee and Wilders ([3]) have studied the influence of interface conditions on the convergence of Krylov-Schwarz domain decomposition methods and showed that an application of a Krylov-type method on the interface problem has no overhead compared to a standard approach but accelerates significantly the convergence speed of the algorithm for all considered transmission condition types. In this work, we are interested in applying this well-established technique to nonlinear time-dependent problems in order to benefit from its accelerating properties known in the linear context. Optimized Schwarz Waveform relaxation for the advection-diffusion equation have been implemented as a preconditioner, for a Krylov method for the interface problem presented in §4, in [1].

The present paper proposes a new space-time parallel algorithm for the Nonlinear Reactive Transport. It relies on the interpretation of the Schwarz algorithm as a Jacobi algorithm for the space-time interface problem. This interface problem can in turn be solved by Newton-Krylov or Krylov-Newton space-time methods. We present two of those methods. For sake of simplicity, the presentation is made in the case of two subdomains.

The paper is organised as follows: In section 2 we set up the problem to solve. In section 3 we describe the Schwarz waveform relaxation algorithm. In section 4 the reduction to the interface variables is presented. The two new approaches are described in section 5. Numerical issues as implementation details and the used framework as well as numerical results in 2D and 3D are given in section 6. Finally in section 7, we present a test-case developed in the industrial platform Arcane, involving space-time adaptation of the classical approach.

## 2 Problem Description

We consider the model problem of a coupled two-species reactive transport system

$$\begin{aligned} \partial_t(\phi u) + \operatorname{div}(-a\nabla u + bu) & -R(u, v) = f_u & \text{on } \Omega \times [0, T], \\ \partial_t(\phi v) & +R(u, v) = f_v & \text{on } \Omega \times [0, T], \end{aligned} \quad (2.1)$$

The spatial domain is  $\Omega \subset \mathbb{R}^d$ ,  $d = 1, 2, 3$  and the simulation period is  $[0, T]$ .  $\phi(x) > 0$  is the porosity of the medium. The mobile species  $u$  is subject to a linear transport, defined by the operator  $Lu := \operatorname{div}(-a\nabla u + bu)$ , including diffusion described by a positive diffusion coefficient  $a > 0$  and advection described by a Darcy field  $b \in \mathbb{R}^d$ . The fixed species  $v$  is coupled to the mobile species  $u$  by a nonlinear coupling term  $R(u, v)$ . Both species are subject to a force, defined by the right hand side terms  $f_u, f_v$ . Initial conditions are given for the mobile and fixed species

$$u(x, 0) = u_0(x), \quad v(x, 0) = v_0(x) \quad \text{on } \Omega, \quad (2.2)$$

and a boundary condition for the mobile species  $u$

$$\mathcal{G}u = g(x, t), \quad \text{on } \partial\Omega \times (0, T], \quad (2.3)$$

where the linear boundary operator  $\mathcal{G}$  can be of different types, e.g. Dirichlet, Neumann.

This problem arises as a subproblem of multispecies reactive transport systems and appears to be the most challenging subsystem since mobile and fixed species are coupled by nonlinear reaction terms resulting of kinetic reactions. In [16], S. Kräutle shows that, after reducing a general multispecies reactive transport systems with kinetic and equilibrium reactions, the resulting nonlinearly coupled equations are of the same type as system (2.1). He also established the well-posedness of the problem.

For the sake of readability of the forthcoming analysis, we will use the following notation to concentrate the problem defined by equations (2.1, 2.2, 2.3):

$$\begin{aligned} \partial_t(\phi w) + \mathcal{L}w + \mathcal{F}(w) &= f_w && \text{on } \Omega \times [0, T], \\ w(x, 0) &= w_0(x) && \text{on } \Omega, \\ \mathcal{J}w &= g(x, t) && \text{on } \partial\Omega \times (0, T]. \end{aligned} \tag{2.4}$$

By setting  $w = (u, v)$ ,  $\mathcal{F}(\cdot) = (-R(\cdot), R(\cdot))$ ,  $f_w = (f_u, f_v)$ ,  $w_0 = (u_0, v_0)$ ,  $\mathcal{J} = \mathcal{G}\Pi_u$  and  $\mathcal{L}w = (Lu, 0)$ , one obtains problem (2.1, 2.2, 2.3) within formulation (2.4). Problem (2.4) is much more general and can easily be extended to other class of problems. Keep in mind that  $\mathcal{L}$  is the linear elliptic operator, and  $\mathcal{F}$  is the nonlinear operator.

### 3 The Schwarz Waveform Relaxation Algorithm

We decompose the domain  $\Omega$  into two non-overlapping domains  $\Omega_1$  and  $\Omega_2$  and call the common boundary  $\Gamma = \overline{\Omega}_1 \cap \overline{\Omega}_2$  the interface. We introduce the following Schwarz waveform relaxation algorithm to approximate the solution of (2.4): Suppose the iterates  $w_1^{k-1}$  and  $w_2^{k-1}$  to be given, then one step of the algorithm consists in solving for both subdomains  $i = 1, 2$

$$\begin{aligned} \partial_t(\phi w_i^k) + \mathcal{L}w_i^k + \mathcal{F}(w_i^k) &= f_w && \text{on } \Omega_i \times [0, T], \\ w_i^k(x, 0) &= w_0(x) && \text{on } \Omega_i, \\ \mathcal{J}w_i^k &= g(x, t) && \text{on } (\partial\Omega_i \setminus \Gamma) \times (0, T], \\ \mathcal{B}_i w_i^k &= \mathcal{B}_i w_{3-i}^{k-1} && \text{on } \Gamma \times [0, T]. \end{aligned} \tag{3.1}$$

Note that for the sake of readability we do not introduce additional indices for the right hand side source term  $f_w$  of the transport equation and the initial and boundary conditions  $w_0$  and  $g$  in  $\Omega_i$ . To finish the definition of the algorithm, we provide an initial guess  $w_i^0$ . This initial guess could be the result of a computation on a coarser grid. The interface transmission operators  $\mathcal{B}_i$ ,  $i = 1, 2$  are linear operators. Different choices are conceivable, we limit our developments here to linear differential operators of Robin type, i. e.

$$\mathcal{B}_i = \partial_{n_i} + p,$$

with  $n_i$  the unit outward normal of  $\Omega_i$  on  $\Gamma$  and  $p \in \mathbb{R}$ ,  $p > 0$  a constant. The convergence of the algorithm for the linear problem was proved in [10]. As for the nonlinear problem, the convergence can be proved using the tools in [5]. Other transmission conditions have been considered in those two works, using second order Ventcell operators for instance, but not in the nonlinear context yet. The parameter  $p$  can be defined

for two subdomains such as to minimize the convergence factor of the linearized problem. A full theory was set in [11] in the case of semilinear term  $R(u, v) = k(v - \Psi(u))$  see (6.1), linearized into  $R(u, v) = k(v - cu)$ . In this work, we use the same  $p$  across the subdomains, but they also can be chosen different in different subdomains, improving the convergence of the algorithm, see [7].

## 4 The Classical Approach: A Fixed Point Algorithm for the Interface Problem

It is possible to reduce algorithm (3.1) to the so-called interface variables. Define the operator

$$\mathcal{M}_i : (\lambda, f) \mapsto w_i \text{ solution of } \begin{cases} \partial_t(\phi w_i) + \mathcal{L}w_i + \mathcal{F}(w_i) = f_w & \text{on } \Omega_i \times [0, T], \\ w_i(x, 0) = w_0(x) & \text{on } \Omega_i, \\ \mathcal{J}w_i = g(x, t) & \text{on } (\partial\Omega_i \setminus \Gamma) \times (0, T], \\ \mathcal{B}_i w_i = \lambda & \text{on } \Gamma \times [0, T], \end{cases}$$

where  $f = (f_w, w_0, g)$  represents all source terms excepting the ones on the interface that are represented separately by  $\lambda$ . Define the interface variable at iteration  $k$  by

$$\lambda_i^k := (\partial_{n_i} + p)w_i^k.$$

Owing to the transmission conditions of algorithm (3.1) on the interface and the relation

$$n_1 = -n_2,$$

we obtain for  $i \neq j$ ,

$$\lambda_i^{k+1} = (\partial_{n_i} + p)w_i^{k+1} = (\partial_{n_i} + p)w_j^k = -(\partial_{n_j} + p)w_j^k + 2pw_j^k = -\lambda_j^k + 2p\mathcal{M}_j(\lambda_j^k, f).$$

Algorithm (3.1) can therefore be rewritten as

$$\begin{aligned} \lambda_1^k &= -\lambda_2^{k-1} + 2p\mathcal{M}_2(\lambda_2^{k-1}, f), \\ \lambda_2^k &= -\lambda_1^{k-1} + 2p\mathcal{M}_1(\lambda_1^{k-1}, f). \end{aligned} \quad (4.1)$$

The Schwarz algorithm (3.1) is therefore a fixed point algorithm for the interface problem

$$\begin{pmatrix} \lambda_1 \\ \lambda_2 \end{pmatrix} = \begin{pmatrix} -\lambda_2 + 2p\mathcal{M}_2(\lambda_2, f) \\ -\lambda_1 + 2p\mathcal{M}_1(\lambda_1, f) \end{pmatrix}. \quad (4.2)$$

In a linear context, suppose the operator  $\mathcal{F}(\cdot)$  to be linear, the operator  $\mathcal{M}_i$  is linear in both arguments and the algorithm (3.1) is the Jacobi method applied to the linear system

$$\begin{pmatrix} \text{Id} & \text{Id} - 2p\mathcal{M}_2(\cdot, 0) \\ \text{Id} - 2p\mathcal{M}_1(\cdot, 0) & \text{Id} \end{pmatrix} \cdot \begin{pmatrix} \lambda_1 \\ \lambda_2 \end{pmatrix} = \begin{pmatrix} 2p\mathcal{M}_2(0, f) \\ 2p\mathcal{M}_1(0, f) \end{pmatrix}, \quad (4.3)$$

where Id denotes the identity operator. Krylov subspace acceleration can be done by solving the linear interface problem by a Krylov type method like GMRES or CG instead of using a splitting method like Jacobi or Gauß-Seidel (cf. [23]).

Note finally, that the interface variables are time-space variables, i. e. they represent the transmission values on the entire interface for both subdomains globally in time.

## 5 The New Approach

In the nonlinear context, i. e.  $\mathcal{F}(\cdot)$  is nonlinear, the algorithm described on the interface variables by (4.1) is equivalent to the application of a ‘‘bloc-wise’’ fixed point iteration method for the nonlinear system (4.3). Note that the operators  $\mathcal{M}_i$  are nonlinear. We use an iterative method (Newton’s method for instance) in order to realise them.

### 5.1 Schwarz-Newton-Krylov or Nested Iteration Approach

The first approach consists in treating system (4.2) by a Newton-Krylov approach. We seek the zeros of the nonlinear function

$$\Psi(\lambda) := \begin{pmatrix} -\lambda_2 + 2p\mathcal{M}_2(\lambda_2, f) \\ -\lambda_1 + 2p\mathcal{M}_1(\lambda_1, f) \end{pmatrix} - \begin{pmatrix} \lambda_1 \\ \lambda_2 \end{pmatrix}.$$

One step  $n \rightarrow n + 1$  of Newton’s method consists in solving the linear system

$$\Psi'(\lambda^n) \cdot (\lambda^{n+1} - \lambda^n) = -\Psi(\lambda^n).$$

The derivative of  $\Psi$  is given by

$$\Psi'(\cdot) = \begin{pmatrix} -\text{Id} & -\text{Id} + 2p\partial_\lambda \mathcal{M}_2(\cdot, f) \\ -\text{Id} + 2p\partial_\lambda \mathcal{M}_1(\cdot, f) & -\text{Id} \end{pmatrix}.$$

Owing to the definition of a linearised operator

$$\begin{aligned} \mathcal{M}_i^{\text{lin}} : (A, h, f) &\mapsto w_i \\ \text{solution of } \begin{cases} \partial_t \phi w_i + \mathcal{L}w_i + Aw_i = f_w & \text{on } \Omega_i \times [0, T], \\ w_i(x, 0) = w_0(x) & \text{on } \Omega_i, \\ \mathcal{J}w_i = g(x, t) & \text{on } (\partial\Omega_i \setminus \Gamma) \times (0, T], \\ \mathcal{B}_i w_i^{k+1} = h & \text{on } \Gamma \times [0, T], \end{cases} \end{aligned} \quad (5.1)$$

one can state the derivative

$$\Psi'(\cdot) = \begin{pmatrix} -\text{Id} & -\text{Id} + 2p\mathcal{M}_2^{\text{lin}}(\mathcal{F}'(\mathcal{M}_2(\lambda_2^n, f)), \cdot, 0) \\ -\text{Id} + 2p\mathcal{M}_1^{\text{lin}}(\mathcal{F}'(\mathcal{M}_1(\lambda_1^n, f)), \cdot, 0) & -\text{Id} \end{pmatrix}.$$

The entire procedure of the approach is then described by the following algorithm:

**INPUT:**  $\lambda^0$  (initial guess),  $\varepsilon$  (precision),  $n_{\text{max}}$  (maximum iterations)

**RETURN:**  $\lambda$  (solution)

$n = 0$

**repeat**

  // Set up RHS

**if**  $n = 0$  **then**

    No previous iterate is available, use the previous time step as initial guess for the actual time step during evaluation of operators  $\mathcal{M}_i$

**else**

    Use the previous iterate globally in time as initial guess during the evaluation of operators  $\mathcal{M}_i$

**end if**

$$-\Psi(\lambda^n) = \begin{pmatrix} \lambda_1^n + \lambda_2^n - 2p\mathcal{M}_2(\lambda_2^n, f) \\ \lambda_1^n + \lambda_2^n - 2p\mathcal{M}_1(\lambda_1^n, f) \end{pmatrix}$$

// Solve the linear system  $\Psi'\delta_{\lambda^n} = -\Psi(\lambda^n)$  with a Krylov-type method

**for every Krylov-iteration  $k$  do**

realise a Matrix-vector multiplication by

$$\Psi'\delta_{\lambda^n}^k = \begin{pmatrix} -\delta_{\lambda_1^n}^k - \delta_{\lambda_2^n}^k + 2p\mathcal{M}_2^{\text{lin}}(\mathcal{F}'(\mathcal{M}_2(\lambda_2, f)), \delta_{\lambda_2^n}^k, 0) \\ -\delta_{\lambda_1^n}^k - \delta_{\lambda_2^n}^k + 2p\mathcal{M}_1^{\text{lin}}(\mathcal{F}'(\mathcal{M}_1(\lambda_1, f)), \delta_{\lambda_1^n}^k, 0) \end{pmatrix}$$

**end for**

// Update variables

$$\lambda^{n+1} = \lambda^n + \delta_{\lambda^n}$$

$$n = n + 1$$

**until**  $n = n_{\text{max}}$  **or**  $\|\delta_{\lambda^n}\| < \varepsilon$  **or**  $\|b\| < \epsilon$

$$\lambda = \lambda^n$$

The approach requires in every iteration of the outer loop (indices in  $n$ ) to set up a right hand side-vector that demands to solve two nonlinear problems in the subdomains. Therefore, a nested iterative procedure is necessary (Newton for instance), for this reason, we call this approach "Nested Iteration Approach" (NIA) due to the split iterative approaches of the nonlinear interface problem and the nonlinear subproblems. The name "Schwarz-Newton-Krylov" can be used in order to explain the order of application of the different tools: The global problem is first attacked by a Schwarz-type domain-decomposition method. The resulting nonlinear interface problem is attacked by a Newton-type method where, at every iteration, the resulting linear system is solved by a Krylov-type method. Unfortunately, the name "Newton-Krylov-Schwarz" has already been widely used for another type of methods and therefore "Schwarz-Newton-Krylov" may be confusing. On these methods for stationary problems, see [15].

## 5.2 Newton-Schwarz-Krylov or Common Iteration Approach

The second approach is not based on the nonlinear interface problem but attacks the global problem (2.4) up from the beginning. We apply Newton's method on this system and solve in every iteration  $n \rightarrow n + 1$  the linear system

$$\begin{aligned} (\partial_t \phi + \mathcal{L} + \mathcal{F}'(w^n))(w^{n+1} - w^n) &= -(\partial_t w^n + \mathcal{L}w^n + \mathcal{F}(w^n) - f_w) && \text{on } \Omega \times [0, T], \\ w^{n+1}(x, 0) &= w_0(x) && \text{on } \Omega, \\ \mathcal{J}(w^{n+1} - w^n) &= -\mathcal{J}w^n + g(x, t) && \text{on } \partial\Omega \times (0, T], \end{aligned}$$

which can be reformulated to

$$\begin{aligned} (\partial_t \phi + \mathcal{L} + \mathcal{F}'(w^n))w^{n+1} &= \mathcal{F}'(w^n)w^n - \mathcal{F}(w^n) + f_w && \text{on } \Omega \times [0, T], \\ w^{n+1}(x, 0) &= w_0(x) && \text{on } \Omega, \\ \mathcal{J}(w^{n+1}) &= g(x, t) && \text{on } \partial\Omega \times (0, T], \end{aligned}$$

owing to the linearity of the operators  $\mathcal{L}$  and  $\mathcal{J}$ .

We apply then the domain decomposition method on this linear system as we have done in section 3 and reduce the problem to the interface variables. Note that no

further iteration index has to be introduced for the domain decomposition algorithm since no numerical method has yet been assigned to the resulting linear interface problem. The resulting linear problem for every iteration is then given by

$$\begin{pmatrix} \text{Id} & \text{Id} - 2p \mathcal{M}_2^{\text{lin}}(\mathcal{F}'(w_2^n), \cdot, 0) \\ \text{Id} - 2p \mathcal{M}_1^{\text{lin}}(\mathcal{F}'(w_1^n), \cdot, 0) & \text{Id} \end{pmatrix} \cdot \begin{pmatrix} \lambda_1^{n+1} \\ \lambda_2^{n+1} \end{pmatrix} = \\ = \begin{pmatrix} 2p \mathcal{M}_2^{\text{lin}}(\mathcal{F}'(w_2^n), 0, (\mathcal{F}'(w_2^n)w_2^n - \mathcal{F}(w_2^n) + f_w, w_0, g)) \\ 2p \mathcal{M}_1^{\text{lin}}(\mathcal{F}'(w_1^n), 0, (\mathcal{F}'(w_1^n)w_1^n - \mathcal{F}(w_1^n) + f_w, w_0, g)) \end{pmatrix}.$$

Logically, the values for  $(u_1^n, u_2^n)$  that are needed to evaluate the RHS and the matrix-vector multiplication at every iteration have to be provided by a nonlinear solution with operators  $\mathcal{M}_i(\lambda_i^n, f)$ . By giving an initial guess also for the first iterate  $(w_1^{-1}, w_2^{-1})$ , this procedure can be replaced by calculating the values only by the linearised operators

$$w_i^n = \mathcal{M}_i^{\text{lin}}(\mathcal{F}'(w_i^{n-1}), \lambda_i^n, (\mathcal{F}'(w_i^{n-1})w_i^{n-1} - \mathcal{F}(w_i^{n-1}) + f_w, w_0, g)),$$

because, suppose the solution has converged, the linearised operator gives the same solution as the nonlinear operator.

The entire procedure of the approach is then described by the following algorithm:

**INPUT:**  $\lambda^0$ ,  $(w_1^{-1}, w_2^{-1})$  (initial guess),  $\varepsilon$  (precision),  $n_{\max}$  (maximum iterations)

**RETURN:**  $\lambda$  (solution)

$n = 0$

**repeat**

*// Update subdomain solutions*

$$w_1^n = \mathcal{M}_1^{\text{lin}}(\mathcal{F}'(w_1^{n-1}), 0, (\mathcal{F}'(w_1^{n-1})w_1^{n-1} - \mathcal{F}(w_1^{n-1}) + f_w, w_0, g))$$

$$w_2^n = \mathcal{M}_2^{\text{lin}}(\mathcal{F}'(w_2^{n-1}), 0, (\mathcal{F}'(w_2^{n-1})w_2^{n-1} - \mathcal{F}(w_2^{n-1}) + f_w, w_0, g))$$

*// Set up RHS*

$$b = \begin{pmatrix} 2p \mathcal{M}_2^{\text{lin}}(\mathcal{F}'(w_2^n), 0, (\mathcal{F}'(w_2^n)w_2^n - \mathcal{F}(w_2^n) + f_w, w_0, g)) \\ 2p \mathcal{M}_1^{\text{lin}}(\mathcal{F}'(w_1^n), 0, (\mathcal{F}'(w_1^n)w_1^n - \mathcal{F}(w_1^n) + f_w, w_0, g)) \end{pmatrix}$$

*// Solve the linear system  $A\lambda^{n+1} = b$  with a Krylov-type method*

**for every Krylov-iteration  $k$  do**

realise a Matrix-vector multiplication by

$$A\lambda^{n+1,k} = \begin{pmatrix} \lambda_1^{n+1,k} + \lambda_2^{n+1,k} - 2p \mathcal{M}_2^{\text{lin}}(\mathcal{F}'(w_2^n), \lambda_2^{n+1,k}, 0) \\ \lambda_1^{n+1,k} + \lambda_2^{n+1,k} - 2p \mathcal{M}_1^{\text{lin}}(\mathcal{F}'(w_1^n), \lambda_1^{n+1,k}, 0) \end{pmatrix}$$

**end for**

*// Update variables*

$$\delta_{\lambda^n} = \lambda^{n+1} - \lambda^n$$

$$n = n + 1$$

**until**  $n = n_{\max}$  **or**  $\|\delta_{\lambda^n}\| < \varepsilon$

$$\lambda = \lambda^n$$

The approach requires in every iteration of the outer loop (indices in  $n$ ) to set up a right hand side-vector that demands to solve two linear problems in the subdomains. Moreover, in the matrix-vector multiplication inside the Krylov-method, only linear

problems in the subdomains are evaluated. No nested nonlinear iterative method is needed. For this reason and in contrast to the first approach, we call this approach "Common Iteration Approach" (CIA) due to the common iterative approach of the nonlinear character of the monodomain problem. The name "Newton-Schwarz-Krylov" can be used in order to explain the order of application of the different numerical tools: The global problem is first attacked by a Newton-type method. At every iteration, the resulting linear problem is decomposed by a Schwarz-type algorithm where the problem is reduced to the interface variables. The resulting linear system is then solved by a Krylov-type method. As in the first case, we recommend not to use this name as the name "Newton-Krylov-Schwarz" has already been used for another type of methods.

## 6 Numerical Approach

Krylov-subspace accelerators for the linear case have become very popular because they are easy to implement and have no significant overhead compared to a standard approach for the Schwarz domain decomposition algorithm. In the nonlinear case, they are as easy to implement as in the linear case: Once the nonlinear solver for a problem in a subdomain is available, the effort for adding the linearised solver and the implementation of the matrix-vector multiplication and the right hand side vector is negligible. Moreover, in many environments, sophisticated and ready-to-use Krylov-type methods like GMRES or BiCGStab are available.

### 6.1 Implementation

In our prototype code for the two species nonlinear coupled reactive transport system (2.4), the equations are discretised by an implicit Euler scheme in time and a hybrid finite volume scheme (cf. [8]) in space including an upwind advection discretisation and a two-point diffusion discretisation on simple rectangular meshes. Nonlinear problems in the subdomain solver are treated with a global implicit approach by means of Newton's method. The arising linear system is solved by an exact LU-decomposition and convergence of Newton's method is controlled by the residual and the step size with a precision of  $\varepsilon = 10^{-8}$ .

The Classical Approach has been implemented as presented in (4.1). We have implemented both methods, the Nested Iteration Approach and the Common Iteration Approach. Both methods make use of a Krylov-type method, GMRES for instance. In order both approaches to be competitive, we apply a precision strategy in the mood of inexact Newton methods, i. e. in the first iterations of the Newton method, we will not oversolve the linear system and can limit therefore the number of costly subdomain evaluations within a matrix-vector multiplication. The more we advance in the outer Newton iteration, the more precise the linear system has to be solved. The appearing linear system at iteration  $n$  is solved up to a precision of

$$\max \left\{ \min \left\{ \frac{1}{1+n}, \|\Psi(\lambda^n)\| \right\}, 10^{-8} \right\},$$

for the Nested Iteration Approach and

$$\max \left\{ 10^{-1} \cdot \min \left\{ 10^{-n}, \|\delta_{\lambda^n}\| \right\}, 10^{-8} \right\},$$

for the Common Iteration Approach.

Note that the Common Iteration Approach needs to store the discretised values of a solution in both subdomains. This can be viewed as a huge drawback in high performance codes. The Nested Iteration Approach *a priori* does not suffer from this drawback. Anyway, it may be highly desirable to store the solution and use it as initial guess for the evaluation of the right hand side. In practice, using the solution of the previous iterate as initial guess reduces significantly the number of nested Newton iterations in the nonlinear subdomain solver.

Finally, concerning the stopping criterion of the outer Newton iteration, the Nested Iteration Approach can be classically controlled by both the residual and the step size norm. The Common Iteration Approach can though no longer be controlled by the residual norm since we have eliminated that term up from the beginning. Recalculating the residual term afterwards is possible but the cost for this may not be negligible.

## 6.2 The classical approach

We study now the numerical behaviour of the Schwarz waveform relaxation algorithm 3.1. In the first part, we concentrate on issues concerning the influence of the nonlinearity on the performance of the classical approach. In the second part, we compare the classical approach with the two new approaches presented in section 6.3. For the numerical results in this section we fix the time period  $t \in [0, 1]$  and the global domain  $\Omega = [0, 1] \times [0, 1] \in \mathbb{R}^2$ . Discrete steps are  $\Delta t = \Delta x = \Delta y = 2 \cdot 10^{-2}$ . The physical parameters are porosity  $\phi = 1$ , diffusion  $a = 1$ , advection is  $(b_x, b_y) = (1 \cdot 10^{-2}, 5 \cdot 10^{-2})$ . Defining the function

$$f(x, y, t) = (\sin(\pi x) \cos(\pi y) \cos(\pi t) + \cos(\pi x) \sin(\pi y) \cos(\pi t) + \cos(\pi x) \cos(\pi y) \sin(\pi t) + 1)/2,$$

we can set the initial values to  $u_0 = f(x, y, 0)$ ,  $v_0 = f(x, y, 0)/c$  for  $(x, y) \in \Omega$  and we impose Dirichlet boundary conditions with values set to  $u_b(x, y, t) = f(x, y, t)$  for  $(x, y) \in \partial\Omega$ . The function  $f$  provides a heterogeneity in space and time so that we can ensure that the exact solution that we reconstruct numerically does not degenerate to a stationary problem.

We decompose  $\Omega$  into non-overlapping subdomains  $\Omega_1 = [0, 0.5] \times [0, 1]$  and  $\Omega_2 = [0.5, 1] \times [0, 1]$ . We impose a random initial guess on the interface  $\Gamma_1$  in order to ensure the presence of a wide range of possible frequencies in the error.

Therefore we study, as in the linear case, the convergence behaviour of the Schwarz waveform relaxation algorithm with Robin transmission conditions using different parameters  $p$  for the transmission condition. We proceed ten iterations of the algorithm and focus on the resulting error on the interface values which indicate us the numerical performance of the transmission condition with respect to the parameter  $p$ . We study different nonlinear coupling function. First, we consider an adsorption process that is modelled by a BET isotherm law:

$$\Psi(u) = \frac{Q_s K_L u}{(1 + K_L u - K_S u)(1 - K_S u)}. \quad (6.1)$$

BET theory is a rule for the physical adsorption of gas molecules on a solid surface and serves as the basis for an important analysis technique for the measurement of the specific surface area of a material (cf. Brunauer et al. [4]). This law is insofar mathematically interesting as it is neither convex nor concave (cf. figure 6.1).

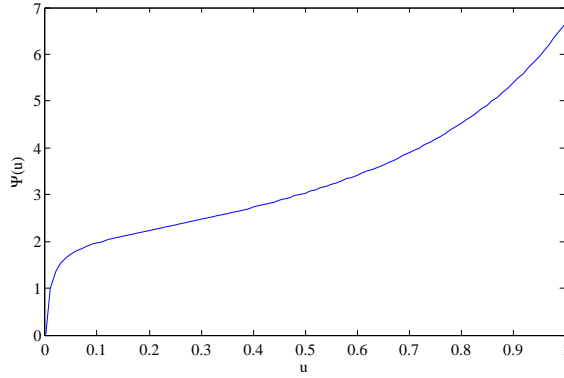


Figure 6.1: BET Isotherm with  $Q_S = 2$ ,  $K_S = 0.7$ ,  $K_L = 100$

The coupling term is given by  $R(u, v) = 100(v - \Psi(u))$  with  $Q_S = 2$ ,  $K_S = 0.7$ ,  $K_L = 100$ .

We study another nonlinear function that is given by an exponential equilibrium model

$$R(u, v) = \exp(10(2v - 3u)) - 1,$$

which models the reaction rate of a kinetic reaction of the form  $2v \rightleftharpoons 3u$  where the forward reaction  $2v \rightarrow 3u$  is much faster than the backward reaction  $2v \leftarrow 3u$ . In this case, we have no asymptotic analysis at hand, and we use the optimised parameter of the single equation of advection-diffusion and the therefore obtained transmission condition behaves well. In figure 6.2 we plot the error at iteration 10 varying the parameter  $p$  of the Robin transmission condition. The square locates the optimised parameter of the linear system established in [11].

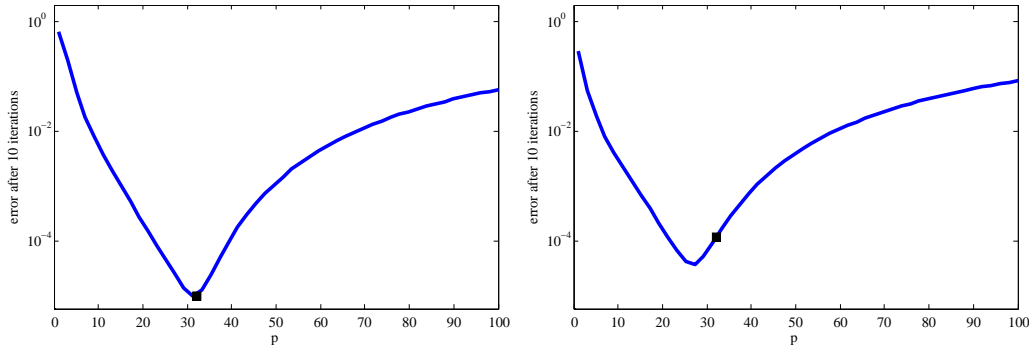


Figure 6.2: Variation of the error of the 10th iterates versus the parameter  $p$  of the Robin transmission condition. Nonlinear function. Left, BET isotherm law, Right, exponential equilibrium model.

In both cases, we observe that the theoretically optimised parameter is close to the best performance for the nonlinear coupled advection-diffusion-reaction system. Tests with other nonlinear functions confirmed this behaviour. The best results are obtained when we have the exact parameter from the linear analysis, that is when the nonlinearity is not too strong.

In the linear case, domain decomposition methods are often used with many subdomains in order to distribute data and computational efforts to several processors. In the nonlinear context, domain decomposition methods can be used in order to localise time step constraints resulting from heterogeneity. In the context of CO<sub>2</sub> geological storage modelling, highly reactive moving fronts appear in the geochemical system. Those regions of strong chemical disequilibrium induce highly localised constraints on the time step using a global implicit approach. If the time step is chosen large, the number of Newton iterations for one time step increases drastically and if the time step is chosen too large, the standard Newton approach fails to converge.

The Schwarz waveform relaxation approach provides the possibility to use different discretisations and numerical approaches in the subdomains. We exploit the possibility to choose different time grids in the subdomains. By this way, we can select a “reactive domain” with small time steps in order to keep the number of Newton iterations for the time steps small. In a “non reactive domain” we can chose much larger time steps and the number of Newton iterations stays acceptable. By this way we can limit the time step restrictions to the area where they appear instead of letting them influence the global time step of the whole simulation domain.

We exemplify this feature with the following test case: the time period is  $[0, 1]$  and the global domain is  $\Omega = [0, 1] \times [0, 1] \in \mathbb{R}^2$ . Discrete steps are  $\Delta x = \Delta y = 2 \cdot 10^{-2}$ . The diffusion parameter is  $\nu = 5 \cdot 10^{-2}$ , advection is  $(b_x, b_y) = (1.5, 1.0)$ . The reaction term is realised by use of the BET isotherm. The initial values are set to  $(u_0, v_0) = (0, 0)$  which is an equilibrium state. We model the entry of a reactive front by imposing a Dirichlet boundary condition on  $x = 0$  with values  $g(x = 0, y, t) = \sin(y\pi)$ . All other boundaries are set to be of no diffusion type, i. e. we impose no concentration gradient on the boundary.

By the incoming reactive front, the chemical system is subject to a strong disequilibrium perturbation. In order the number of Newton iterations not to be too excessive (less than ten), one has to chose a time step of  $10^{-1}$ , i. e. ten time steps. The global monodomain approach has a linear system of 5200 discrete unknowns to solve in every time step and every Newton iteration. The first time step needs 9 Newton iterations to reach convergence, the following time steps (2nd to 10th) need each 7 Newton iterations to reach convergence where we suppose the solution of the previous time step as initial guess of the Newton iteration. We measure the effort of the global approach by the effort of the inversion for one matrix multiplied by the number of matrix inversions since this is the most costly operation. The global effort is hence  $(1 \cdot 9 + 9 \cdot 7) \cdot (5200)^3 = 1.01 \cdot 10^{13}$ .

In a domain decomposition approach, we can chose the reactive subdomain to be  $\Omega_1 = [0, 0.4 + \Delta x] \times [0, 1]$  (2242 discrete unknowns) and the non reactive subdomain to be  $\Omega_2 = [0.4, 1] \times [0, 1]$  (3160 unknowns discrete). Both subdomains have an overlap of one layer of cells. For the reactive subdomain we chose the same time step as in the global monodomain approach, i. e. ten time steps, while for the non reactive subdomain, we can use only one time step without the number of Newton iterations to become important. We impose the initial state as initial guess for the interface values in the Schwarz waveform relaxation iteration and impose the solution of the previous Schwarz waveform relaxation iteration in the Newton iterations. In the first iterate we proceed as in the global approach, i. e. we impose the solution of the previous time step as initial guess for the Newton iterates. In total, we need three Schwarz waveform relaxation iterations in order to reach convergence. In the first iteration, we need for the reactive subdomain 9 iterations in the first time step and

7 iterations for each following time step. In the non reactive subdomain we need 4 iterations. In the second Schwarz iteration, we need 2 iterations for the first 7 time steps and 3 iterations for the last 3 time steps in the reactive subdomain and 3 iterations in the non reactive subdomain. In the third iteration we need 2 iterations for all time steps in the reactive and non reactive subdomains. The total effort is hence  $(1 \cdot 9 + 9 \cdot 7 + 17 \cdot 2 + 3 \cdot 3) \cdot (2242^3) + (4 + 3 + 2) \cdot (3160)^3 = 1.58 \cdot 10^{12}$ . The effort for the domain decomposition solution is hence by a factor of 10 smaller than the effort for a global monodomain solution. Note that this estimation is quite optimistic, since using more performing linear solvers for the linear problems during the Newton iterations may reduce the gain of a domain decomposition approach compared to the global approach.

In figures 6.3 and 6.4 we plot the concentration of  $u$  and  $v$  at  $t = 0.5$  and  $t = 1.0$  at the third iteration of the domain decomposition algorithm.

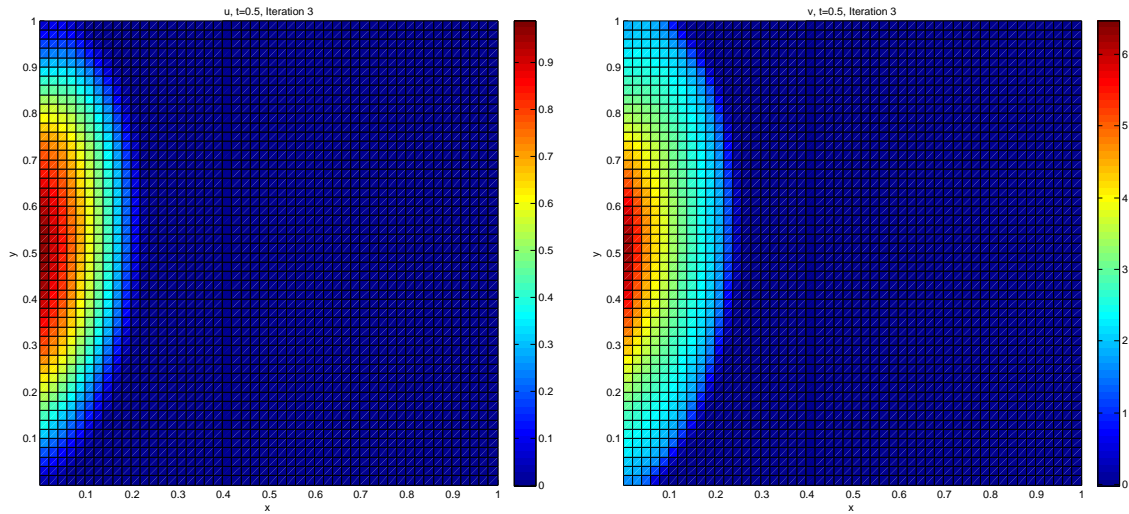


Figure 6.3: Concentration  $u$  and  $v$  at  $t = 0.5$  using the BET isotherm with an incoming reactive front. Solution of the third domain decomposition iteration.

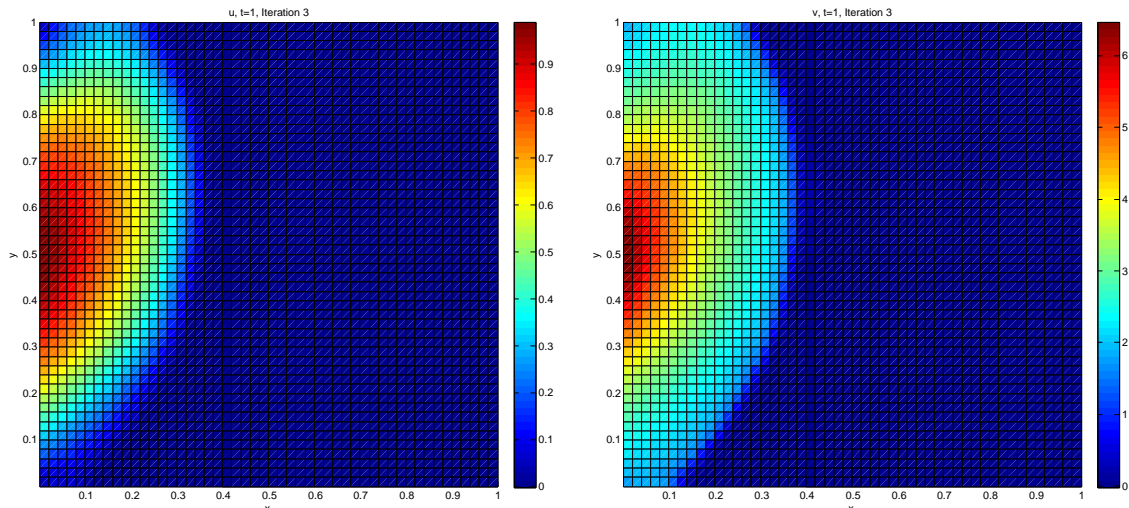


Figure 6.4: Concentration  $u$  and  $v$  at  $t = 1.0$  using the BET isotherm with an incoming reactive front. Solution of the third domain decomposition iteration.

### 6.3 The new approach

We use a similar testing approach as before and set  $k = 100$ ,  $Q_S = 2$ ,  $K_S = 0.7$  and  $K_L = 100$ . Initial values are set to  $(u_0, v_0) = (\frac{1}{2}, \frac{1}{3})$ . By defining the function

$$g(x, y, t) = (\sin(\pi x) \cos(\pi y) \cos(2\pi t) + \cos(\pi x) \sin(\pi y) \cos(2\pi t) + \cos(\pi x) \cos(\pi y) \sin(2\pi t) + 1)/2,$$

we impose Dirichlet boundary conditions with values set to  $u_b(x, y, t) = g(x, y, t)$  for  $(x, y) \in \partial\Omega$ .

In a first time, we are interested in the sensibility of the three approaches with respect to the parameter  $p$  of the Robin transmission condition. We discretise the numerical domain with  $\Delta x = \Delta y = 1/40$  and  $\Delta t = 1/10$  and impose a random initial guess on the interface for the first iteration. As both subdomains have the same size, the number of overall matrix inversions in the linear and nonlinear subdomain solvers for three approaches is a meaningful criterion to measure the numerical performance. We proceed the three approaches for different parameters  $p$  of the Robin transmission condition and plot in figure 6.5 the number of matrix inversions. One observes first that the performance of the classical approach, i. e. a fixed point method on the nonlinear interface problem depends highly on the parameter  $p$  that one chooses for the Robin transmission condition. The best parameter is  $p^* \approx 40$ . The two new approaches, NIA and CIA also show the best performance at  $p^*$  but are much less sensitive to the choice of the parameter. Especially if, in realistic test cases where one has no idea of the best parameter, one underestimates the unknown parameter  $p^*$ , the new approaches do not suffer from the exponential loss of performance. Second, one observes that the CIA is always more performing than the classical and the NIA approach. The NIA is, in a wide range of parameters, more performing than the classical approach but the last one stays more performing in an important range of parameters around the optimal

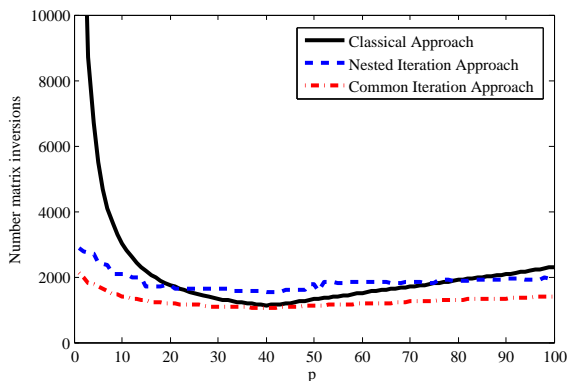


Figure 6.5: Number of matrix inversions versus parameter  $p$  of the Robin transmission conditions for the classical approach (fixed point on the nonlinear interface problem), Nested Iteration Approach and Common Iteration Approach

parameter  $p^*$ . It is well-known for linear problems that the influence of the Robin parameter is less when the Jacobi algorithm corresponding to the classical Schwarz is replaced by a Krylov algorithm. The nonlinear algorithm exhibits the same behaviour.

It turned out that the two new methods, NIA and CIA, have a cost overhead that becomes non negligible if space discretisations are chosen too coarse. For this reason, we study the asymptotic behaviour of the three approaches using always the optimal parameter of the classical approach. We refine the problem in space using always  $\Delta x = \Delta y$ . Note that we keep the time step constant at  $\Delta t = 0.1$ . Refining the discretisation also in time would lead to a problem that is quasi linear at every time step since we use a global implicit approach. The negligible nonlinearity would result in a minimal number of nested Newton iterations and the overhead cost would become more important. We measure again the overall number of matrix inversions in the three approaches. One observes that the overhead cost of the two new approaches compared to the classical approach becomes negligible up from a discretisation with about 150 grid points per dimension for the NIA and about 20 grid points per dimension for the SIA. For problems finer than the respective thresholds, the new approaches are always more performing compared to the classical approach with the best parameter for the transmission condition. Moreover, the finer the discretisation, the larger the problem, the more important the accelerating property of the two new approaches. Note that both new approaches have the same slope of  $O(N^{1/7})$  in the asymptotic behaviour which is considerably less than the slope of the classical approach which behaves like  $O(N^{1/2.75})$ . The vertical translation of the curves for the two new approaches indicates their overhead cost. Again here, a theoretical analysis will be interesting.

In order to exemplify the accelerating property of the two new approaches, we perform a simulation with  $N_x = N_y = 200$  points in each dimension keeping the number of time steps constant and compare the convergence behaviour of the stopping criteria of the three methods. In figure 6.7 we plot the convergence criterion versus the number of matrix inversions. One observes the quadratic convergence of the new approaches since they are Newton-based, the quadratic convergence is observed late in the history since the initial guess (randomly chosen) is far from the exact solution.

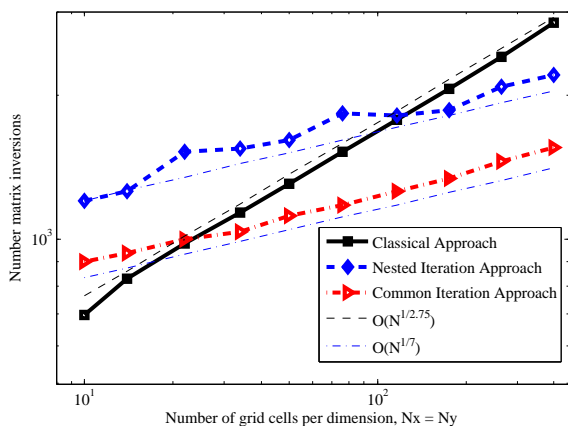


Figure 6.6: Number of matrix inversions versus number of discrete points per dimension ( $N_x = N_y$ ) for the classical approach (fixed point on the nonlinear interface problem), Nested Iteration Approach and Common Iteration Approach

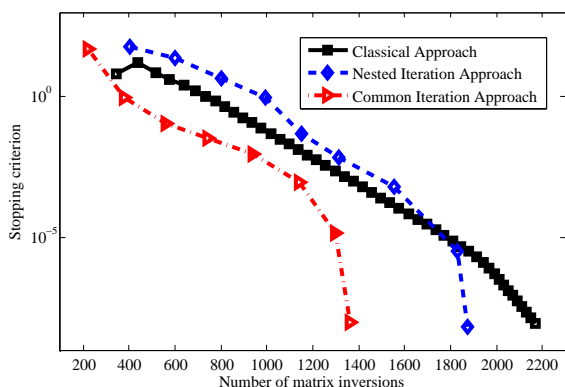


Figure 6.7: Convergence history with 200 points per space dimension for the Classical approach, Nested Iteration Approach and Common Iteration Approach

The classical approach shows only a superlinear convergence, also in this case, the superlinear character appears late in the convergence history.

Finally, we want to apply the two new approaches to a benchmark test case in the context of CO<sub>2</sub> geological storage. The 3D test case is based on the benchmark for the SHPCO<sub>2</sub> project (Simulation haute performance pour le stockage géologique du CO<sub>2</sub>) which is described in [17]. The global domain is set to  $\Omega = [0, 4750] \times [0, 3000] \times [-1100, -1000]$  and is decomposed into the two nonoverlapping subdomains  $\Omega_1 = [1000, 2500] \times [0, 3000] \times [-1050, -1000]$  and  $\Omega_2 = \Omega \setminus \Omega_1$ . We call  $\Omega_1$  the reactive subdomain since in this subdomain an injection of the mobile species  $u$  is modelled by a source term. The initial state is zero for the mobile and immobile species. We consider again the BET isotherm law as nonlinear coupling term. The injected mobile species is partially absorbed by the reaction and partially transported

by mainly advection.

Simulation time is  $[0, 100]$ . As the waveform relaxation approach allows to use different discretisations in the subdomains, we chose to use ten time steps in the reactive subdomain  $\Omega_1$  and only five time steps in the subdomain  $\Omega_2$ . This choice is insofar justified since the rapid injection in the reactive subdomain restricts the time step size by imposing a maximum number of Newton iterates of ten. As in the subdomain  $\Omega_2$ , the mobile species appears only by transport processes on a slower time scale than the injection, one can chose a larger time step in order to respect the maximum number of Newton iterations.

Concerning the parameter of the Robin transmission condition, we use the same as before. The initial guess on the interface is zero for both subdomain interfaces.

In figure 6.8 we plot the convergence histogram, i.e. the stopping criterion in a logarithmic scale versus the CPU time (normalised to the CPU time of the classical approach). Note that both subdomains have a different size of unknowns and therefore

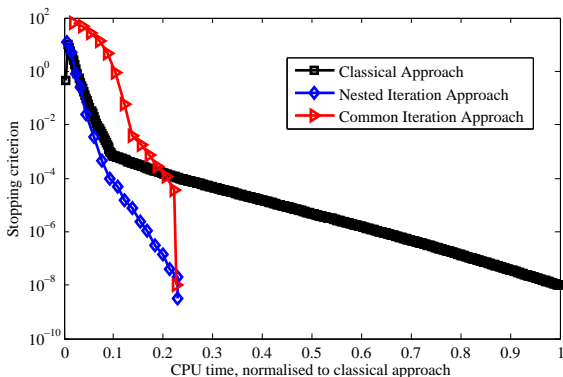


Figure 6.8: Convergence history with 200 points per space dimension for the Classical Approach, Nested Iteration Approach and Common Iteration Approach

the number of matrix inversions, as used in the previous examples, is no longer a valid tool to measure the effort. One observes clearly that the classical approach converges only linearly while the two new approaches show a quadratic convergence. Moreover, the two new approaches need only about 20 percent of the CPU time of the classical approach. Note that the stopping criterion of the Common Iteration Approach seems to crash down in the last iteration as one observes in figure 6.8. This behaviour is due to the fact that the GMRES solver provided in the last iteration the same solution as in the last but one iteration due to the precision strategy. As a consequence, the norm of the variation of the iterates is zero and this indicates that the algorithm has converged. To indicate this behaviour in the plot, we set the convergence criterion of the last iterate to the overall precision  $10^{-8}$ .

In the first test case using the BET isotherm we observed that the Common Iteration Approach is always more performing than the Nested Iteration Approach. However, in the SHPCO2 test case the opposite holds. Note that there is no *a priori* more performing method, all depends on the problem to treat. We performed several tests with different problems and we can state several points:

First, both new approaches, the Nested Iteration Approach and the Common Iteration Approach show always much less sensibility to the parameter of the Robin transmis-

sion condition than the classical approach.

Second, both new approaches show always a more favourable slope in the case of asymptotic mesh refinement in space on the one hand and on the other hand they show always the same slope up to a vertical translation which indicates the different overhead cost.

Third, the question which of both new approaches is more performing on a problem is a challenge between the complexity to solve the problem with a domain decomposition approach and the difficulty to solve it with a nonlinear approach. Problems which are easy to solve with a domain decomposition approach since they are for example quite advective in normal interface direction and less diffusive have concentrated their main challenge in the nonlinearity. This is the case of the SHPCO2 test where the main difficulty lies in the massive injection of mobile species in the reactive domain which induces an elevated number of Newton iterations. The Nested Iteration approach showed to be more performing on this cases where the nonlinearity is the main challenge. On the other hand, for test cases which are difficult to solve with a domain decomposition approach, for example highly diffusive cases like the synthetic case in the previous part, the Common Iteration Approach seems to be more performing.

Altogether, we can summarise that both new approaches are more performing than the classical approach whenever the overhead cost due to coarse discretisations become negligible. Moreover, which one of the new approaches is more performing lies on the challenging character of the problem and can hardly be predicted in advance. Nevertheless, passing from one approach to another is very simple since they only inverse two loops.

## 7 First numerical tests in industrial environment Arcane

The work presented in this article is part of an international project called SHPCO2 (high performance simulation of CO<sub>2</sub> geological storage), initiated by the French National Research Agency (ANR). One part of the project is to study different domain decomposition approaches for multi-species reactive transport problems in the context of high performance computing for CO<sub>2</sub> geological storage simulation. Arcane is the underlying industrial simulation platform for HPC applications which is under co-development of the two national French institutes IFP Energies nouvelles and CEA Energies alternatives, see [10] for specificities.

A first approach of Schwarz Waveform Relaxation methods has been implemented into the Arcane development platform to show the ability to treat these kind of complex problems in a HPC environment. In the context of a domain specific language for parallel finite volumes (cf. [19]), the classical fixed-point iteration type approach as described in equation (4.2) has been implemented. Spatial grids on the interface are conformal but time-stepping can be different in the sub-domains. This allows for individual approaches of combined time-stepping and nonlinearity control in the different sub-domains. Currently, two sub-domains are treated, one which contains most of the non-linear problems due to chemical reactions. The other subdomain is essentially characterised by the absence of strong nonlinearities.

We have tested the approach with the SHPCO2 test case. This synthetic test case contains all major physical and chemical effects which are characteristic for CO<sub>2</sub> geological storage modelling. The full definition of the test case can be found in

[17, 10]. We summarise here the main points of the test case. The two-dimensional geometry contains a pressure-driven meander-shaped flow through areas with high and low porosity (see figure 7.1). At the injector wells a considerably higher pressure is imposed than on the producer well. For the first approach, we have implemented only a two-phase flow including solid and liquid phase. As a consequence, we have modelled the initially gaseous  $\text{CO}_2$  as a solid phase which is dissolved afterwards.

The chemical system is presented as usually by distinction between primary species

$$c = \begin{pmatrix} c_1 \\ c_2 \\ c_3 \\ c_4 \\ c_5 \\ c_6 \\ c_7 \\ c_8 \end{pmatrix} = \begin{pmatrix} H_2O \\ \text{Tracer} \\ \text{CO}_2(aq) \\ \text{Cl}^- \\ \text{H}^+ \\ \text{Na}^+ \\ \text{Ca}^{++} \\ \text{SiO}_2(aq) \end{pmatrix}, \quad q = \begin{pmatrix} q_1 \\ q_2 \end{pmatrix} = \begin{pmatrix} \text{Calcite} \\ \text{Quartz} \end{pmatrix},$$

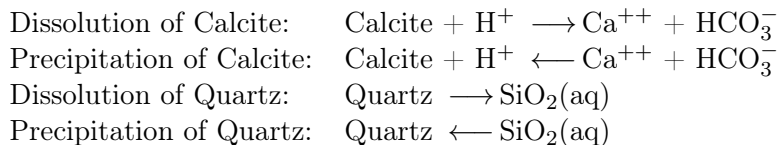
and secondary species

$$x = \begin{pmatrix} x_1 \\ x_2 \end{pmatrix} = \begin{pmatrix} \text{HCO}_3^- \\ \text{OH}^- \end{pmatrix}, \quad z = (z_1) = (\text{CO}_2(\text{solid})).$$

The first group being an independent set of species while the second group forms species whose concentration can be determined by solving the associated equilibrium problem. The equilibrium reactions are represented in a Morel tableau indicating the stoichiometric indices of the associated equilibrium reactions:

	$c_1$	$c_2$	$c_3$	$c_4$	$c_5$	$c_6$	$c_7$	$c_8$	$q_1$	$q_2$
$x_1$	1		1		-1					
$x_2$	1				-1					
$z_1$				1						

Besides the equilibrium reactions, we include four reactions whose reaction speeds are modelled by different kinetic laws:



We simulate the test case on a 2D mesh with 76 cells in  $x$ -direction and 48 cells in  $y$ -direction. The initial subdomains are chosen such as the reactive domain covers the initial  $\text{CO}_2$ -plume and is slightly blown-up. The non-reactive domain contains the part where the system is in chemical equilibrium. Both domains do overlap in the initial state (see figure 7.1). For the interface transmission conditions, we impose Robin conditions with a localised one-dimensional approximation of 0th order of the optimal parameter. The Schwarz waveform relaxation algorithm is applied to a time-window and iteration is proceeded between the sub-domains until the change of the concentration at the end of a time window is smaller than  $10^{-4}$ . We perform a simulation of the first 95.13 years with three equally sized time windows and ten time steps per time window (i. e.  $\Delta t = 3.17$  years). In order to show the localisation

of numerical difficulties related to kinetic reactions appearing mainly in the reactive subdomain, we chose no adaptive time strategy and concentrate on the number of nonlinear steps needed to solve the subdomains. In figure 7.2, we plot the pH-value at the end of the simulation. The initially solid  $\text{CO}_2$  has partially dissolved into the liquid phase where it becomes acid resulting in low pH-values. The associated regions are chemically highly reactive, both from a kinetic and an equilibrium point of view. As a consequence, non-linearities originating from chemistry are concentrated in regions with low pH-value. Note that we have chosen the initial reactive sub-domain such that at the end of the simulation, the reactive domain covers the whole region with low pH-value.

The Schwarz waveform relaxation algorithm needs 2 iterations per time window to converge. The overall number of global nonlinear steps are 421 in the reactive and 306 in the non reactive subdomains. The linear systems during the nonlinear iteration are more difficult to solve in the reactive domain than in the non reactive domain. The iterative solver of GMRES type preconditioned with Hypr's Euclid preconditioner needed overall 10234 iterations in the reactive and only 3806 iterations in the non reactive subdomain. This means, that in the reactive subdomain, the linear solver needed 24.3 iterations in average and in the non reactive domain it needed only 12.4 iterations.

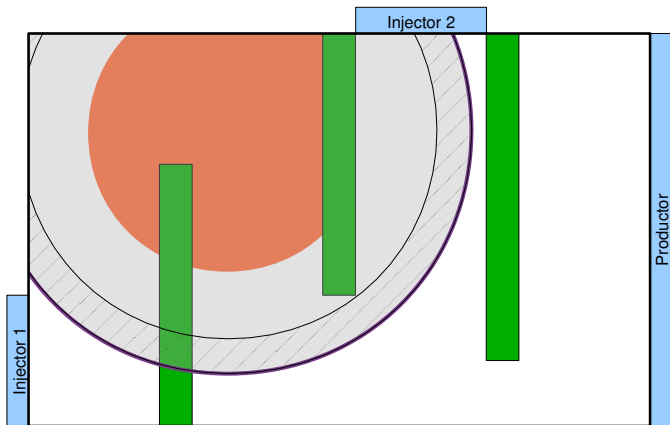


Figure 7.1: Choice of subdomains in the SHPCO2 2D test case. Orange: position of the initially present  $\text{CO}_2$ . Green: Areas with low porosity. Shaded grey: reactive subdomain. Violet solid line: Interface of the reactive subdomain. Hatched annulus: overlapping region between reactive and non reactive subdomain.

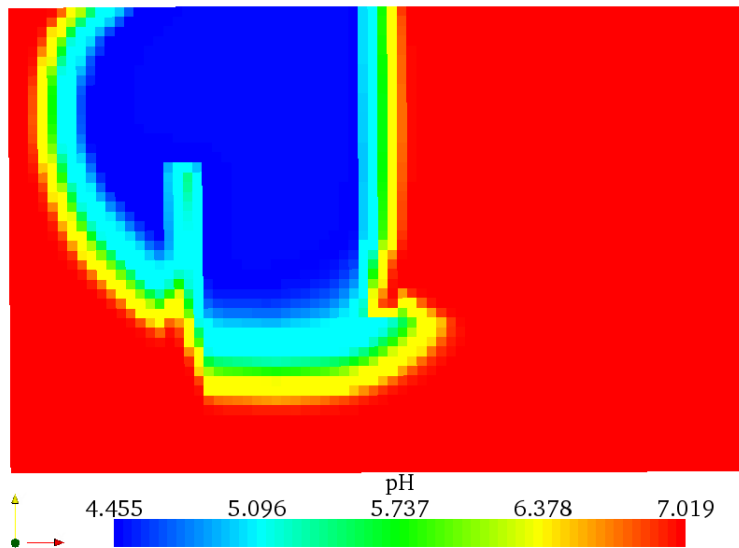


Figure 7.2: pH of the SHPCO2 test case at  $t = 95.13$  years (end of the first time-window for the domain decomposition simulation). The low pH-value can be seen as an indicator of highly-chemically reactive zones.

## 8 Conclusion

Basing on a nonlinear coupled reactive transport system we have developed two new approaches for solving the interface problem in the nonlinear case. The Nested Iteration Approach applies a Newton-Krylov method on the nonlinear interface problem of the Schwarz algorithm. The Common Iteration Approach applies a Newton method on the global problem and solves than in every iteration the appearing linear interface problem of the Schwarz algorithm with a Krylov method. We have implemented and tested both methods. Comparative results with the classical approach that consists in the application of a fixed point method on the nonlinear interface problem have been provided.

The numerical tests showed that, besides an overhead cost for coarse space discretisations, both methods have an accelerating property and show much less sensibility with respect to the choice of the parameter of the Robin condition. The quadratic convergence behaviour of the new approaches outperform the superlinear convergence behaviour of the classical approach. An implementation of the Schwarz waveform relaxation algorithm in a complex industrial case has shown the usefulness of the method. An extension to the new approaches, together with a study of how to reduce the overhead cost will certainly be fruitful.

## References

- [1] D. Bennequin, M. J. Gander, L. Gouarin, and L. Halpern. Optimized schwarz waveform relaxation for advection reaction diffusion equations in two dimensions. Report hal-00986756, 2014.

- [2] P. Bjørstad and O. Widlund. To overlap or not to overlap: A note on a domain decomposition method for elliptic problems. *SIAM Journal on Scientific and Statistical Computing*, 10:1053–1061, 1989.
- [3] E. Brakkee and P. Wilders. The Influence of Interface Conditions on Convergence of Krylov-Schwarz Domain Decomposition for the Advection-Diffusion Equation. *Journal of Scientific Computing*, 12:11–30, 1997.
- [4] S. Brunauer, P. H. Emmett, and E. Teller. Adsorption of Gases in Multimolecular Layers. *Journal American Chemical Society*, 60(2):309–319, 1938.
- [5] F. Caetano, L. Halpern, M. Gander, and J. Szeftel. Schwarz waveform relaxation algorithms for semilinear reaction-diffusion. *Networks and heterogeneous media*, 5(3):487–505, 2010.
- [6] X.-C. Cai and D. E. Keyes. Nonlinearly Preconditioned Inexact Newton Algorithms. *SIAM Journal on Scientific Computing*, 24:183–200, 2000.
- [7] O. Dubois. *Optimized Schwarz Methods for the Advection-Diffusion Equation and for Problems with Discontinuous Coefficients*. PhD thesis, McGill University in Montréal, Canada, 2007.
- [8] R. Eymard, T. Gallouët, and R. Herbin. Discretisation of heterogeneous and anisotropic diffusion problems on general non-conforming meshes, sushi: a scheme using stabilisation and hybrid interfaces. *IMAJNA*, see also <http://hal.archives-ouvertes.fr/docs/00/21/18/28/PDF/suchi.pdf>, 2008.
- [9] M. J. Gander. A waveform relaxation algorithm with overlapping splitting for reaction diffusion equations. *Numer. Linear Alg. Appl.*, 6:125–145, 1998.
- [10] F. Häberlein. *Time-Space Domain Decomposition Methods for Reactive Transport Applied to CO<sub>2</sub> Geological Storage*. PhD Thesis, University Paris 13, 2011.
- [11] F. Häberlein and L. Halpern. Optimized Schwarz waveform relaxation for non-linear systems of parabolic type. In J. Erhel, M. Gander, L. Halpern, G. Pichot, T. Sassi, and O. B. Widlund, editors, *Domain Decomposition Methods in Science and Engineering XXI*, volume 98 of *Lect. Notes Comput. Sci. Eng.*, pages 27–38. Springer, 2015.
- [12] F. Häberlein, L. Halpern, and A. Michel. Schwarz waveform relaxation and Krylov accelerators for nonlinear reactive transport. In R. E. Bank, M. J. Holst, O. B. Widlund, and J. Xu, editors, *Domain Decomposition Methods in Science and Engineering XX*, pages 409–416. Springer, 2013.
- [13] L. Halpern. Optimized Schwarz waveform relaxation: roots, blossoms and fruits. In *Domain Decomposition Methods in Science and Engineering XVIII*, volume 70 of *Lect. Notes Comput. Sci. Eng.*, pages 225–232. Springer, 2009.
- [14] L. Halpern, C. Japhet, and J. Szeftel. Optimized Schwarz waveform relaxation and discontinuous Galerkin time stepping for heterogeneous problems. *SIAM J. on Numer. Anal.*, 50(5):2588–2611, 2012.
- [15] D. Knoll and D. Keyes. Jacobian-free Newton-Krylov methods: a survey of approaches and applications. *J. of Comp. Phys.*, 193:357–397, 2004.
- [16] S. Kräutle. *General Mutli-Species Reactive Transport Problems in Porous Media: Efficient Numerical Approaches and Existence of Global Solutions*. Habilitation thesis, University of Erlangen-Nuremberg, March 2008.

- [17] A. Michel, F. Haeberlein, and L. Trenty. Cas Tests SHPCO2 n°3 — Test synthétique pour le transport réactif dans le cadre du stockage géologique de CO2. 2009.
- [18] S. Ovtchinnikov and X.-C. Cai. One level Newton-Krylov-Schwarz algorithm for unsteady non-linear radiation diffusion problem. *Numer. Linear Algebra Appl.*, 11, 2004.
- [19] C. Prud’Homme, D. A. Di Pietro, J.-M. Gratien, F. Häberlein, and A. Michel. Basic concepts to design a DSL for Parallel Finite Volume Applications. In *POOSC '09 - 8th workshop on Parallel/High-Performance Object-Oriented Scientific Computing*, pages 3:1–11, Genova, Italy, July 2009. ACM.
- [20] A. Quarteroni and A. Valli. *Domain Decomposition Methods for Partial Differential Equations*. Oxford Science Publications, London, 1999.
- [21] Y. Saad and M. Schultz. GMRES: A generalized minimal residual algorithm for solving nonsymmetric linear systems. *SIAM J. Sci. Stat. Comput.*, 7(3):856–869, 1986.
- [22] B. F. Smith, P. E. Bjørstad, and W. Gropp. *Domain Decomposition: Parallel Multilevel Methods for Elliptic Partial Differential Equations*. Cambridge University Press, Cambridge, 1996.
- [23] A. Toselli and O. Widlund. *Domain decomposition methods—algorithms and theory*. Springer Verlag, 2005.
- [24] H. Van der Vorst. Bi-CGSTAB: A fast and smoothly converging variant of Bi-CG for the solution of nonsymmetric linear systems. *SIAM Journal on scientific and Statistical Computing*, 13:631, 1992.